Arabian Journal of Chemistry (2023) **16**, 104479

King Saud University

Arabian Journal of Chemistry

www.ksu.edu.sa
www.sciencedirect.com

ORIGINAL ARTICLE

Novel 1,3,4-oxadiazole thioether and sulfone derivatives bearing a flexible *N*-heterocyclic moiety: Synthesis, characterization, and anti-microorganism activity

Fang Wang, Bin-Xin Yang, Tai-Hong Zhang, Qing-Qing Tao, Xiang Zhou *, Pei-Yi Wang, Song Yang *

State Key Laboratory Breeding Base of Green Pesticide and Agricultural Bioengineering, Key Laboratory of Green Pesticide and Agricultural Bioengineering, Ministry of Education, Center for R and D of Fine Chemicals of Guizhou University, Guiyang 550025, China

Received 1 July 2022; accepted 28 November 2022
Available online 5 December 2022

KEYWORDS

1, 3, 4-oxadiazole derivatives;
Thioether derivatives;
Sulfone derivatives;
Antibacterial activity

Abstract In the search for more efficient and versatile anti-phytopathogen agents, a series of new 1,3,4-oxadiazole thioether/sulfone analogues bearing a flexible *N*-containing heterocyclic pattern were elaborately prepared, and their bioactivities against plant pathogenic microorganisms were systematically evaluated. Bioassay screening results demonstrated that compounds **32** and **33** significantly inhibited the growth of *Xanthomonas oryzae* pv. *oryzae* (*Xoo*) *in vitro* (**32**, EC_{50} = 5.17 mg L^{-1}; **33**, EC_{50} = 1.19 mg L^{-1}), which were significantly surpass commercial bismerthiazol (**BT**) and thiodiazole copper (**TC**). Meanwhile, pot experiments confirmed the prospective applications of compound **33** in managing rice bacterial leaf blight and its good safety toward rice plants. Further studies showed that compound **33** interfered with the formation of bacterial biofilms and inhibited bacterial virulence factors. Furthermore, an *in vitro* antifungal bioassay showed that compound **32** possessed remarkable growth inhibitory activity against *Sclerotinia sclerotiorum* (*S.s.*, EC_{50} = 22.16-mg L^{-1}) and *Verticillium dahlia* (*V.d.* EC_{50} = 32.78 mg L^{-1}). These results all confirmed that the designed 1,3,4-oxadiazole compounds displayed potential for managing plant microbial diseases through targeting dihydrolipoamide S-succinyltransferase (DLST).

* Corresponding authors.
E-mail addresses: zhoux1534@163.com (X. Zhou), jhzx.msm@gmail.com (S. Yang).

Peer review under responsibility of King Saud University.

Production and hosting by Elsevier

https://doi.org/10.1016/j.arabjc.2022.104479
1878-5352 © 2022 The Author(s). Published by Elsevier B.V. on behalf of King Saud University.

1. Introduction

Plant diseases have attracted global attention owing to the substantial economic losses caused in agriculture (Bauske et al., 2018; Guo et al., 2021). According to statistics, about 16 %–20 % of economic crop losses globally are due to preharvest plant disease (Savary et al., 2019). Notably, rice bacterial leaf blight is an intractable plant bacterial disease that caused by *Xanthomonas oryzae* pv. *oryzae* (*Xoo*) and leading to reducing yields in rice-growing countries as high as 10 %–50 % per year (Lu et al., 2014). Therefore, improving the grain yield and quality has become a critical issue for agriculture worldwide. Disease prevention is an important measure for ensuring steady increases in food production, with the use of agrochemicals currently being the most important, low-cost, and effective method. However, some problems, such as environmental pollution and drug resistance have inevitably developed with the long-term use and abuse of agrochemicals, seriously restricting the production and development of modern agriculture (Fisher et al., 2018, Gould et al., 2018, Velema et al., 2013). The use/overuse of commercially bismerthiazol has already leading to the occurrence of bismerthiazol-resistant *Xoo* strain. Therefore, rising crisis of bactericide resistance urges the excavation of agrochemicals with novel action modes.

Nitrogen-containing heterocyclic compounds are considered potential sources of natural products for the development of new drugs (Benedik, 1998). Examples, such as oxadiazoles, triazoles, pyridines, indoles, and their derivatives, are commonly used as medicines and pesticides (Gan et al., 2017). Among them, 1,3,4-oxadiazole derivatives have gained attention not only for their significant biological abilities, including antiviral (Wang et al., 2016), antifungal, insecticidal (Formagio et al., 2008), antibacterial (Li et al., 2013, Xu et al., 2011; Wang et al., 2018), and antitumor activities (Huang et al., 1987), but also for their good selectivity, high activity, and low toxicity. And representative 1,3,4-oxadiazole derivatives were summarized and listed in Table S1. In particular, 1,3,4-oxadiazole analogues exhibit broad-spectrum bioactivities in agriculture, with some related commercial pesticides successfully developed, such as herbicide oxadiazon, herbicide oxadiargyl, and insecticide metoxadiazone (Tao et al., 2019). Therefore, the 1,3,4-oxadiazole scaffold is an important pharmacophore group in agrochemical research and development. In our previous studies, many series of 2,5-disubstituted-1,3,4-oxadiazole thioether/sulfone analogues with a rigid group at the 2-position of the 1,3,4-oxadiazole were successfully synthesized, with some target molecules showing excellent bioactivity against phytopathogens (Zhu et al., 2019, Wang et al., 2016, Chen et al., and Xiang et al., 2020). Among them, commercial candidate pesticides Jiahuangxianjunzuo and Fubianezuofeng have been developed, and valuable experience in structural modification gained (Su et al., 2016; Wu et al., 2021). For example, we found that sulfone derivatives increased adenosine triphosphate (ATP) levels and acted as a covalent inhibitor in an anti-dihydrolipoamide *S*-succinyltransferase (DLST) function study (Chen et al., 2019; Chen et al., 2020).

Encouraged by the aforesaid observations and as a continuation of our research efforts, three series of 1,3,4-oxadiazole thioether/sulfone analogues bearing a flexible *N*-containing six-membered heterocyclic moiety, such as piperazine, piperidine, and morpholine, at the 2-position of the 1,3,4-oxadiazole ring were designed (Fig. 1) and synthesized (Figs. 2-4). All obtained compounds were systematically investigated for their *in vitro* anti-microorganism potency against three plant pathogenic bacteria, namely, *Xanthomonas oryzae* pv. *oryzae* (*Xoo*), *Xanthomonas axonopodis* pv. *citri* (*Xac*), and *Pseudomonas syringae* pv. *actinidiae* (*Psa*), and six plant pathogenic fungi, namely, *Gibberella zeae* (*G.z.*), *Botryosphaeria dothidea* (*B.d.*), *Fusarium oxysporum* (*F.o.*),

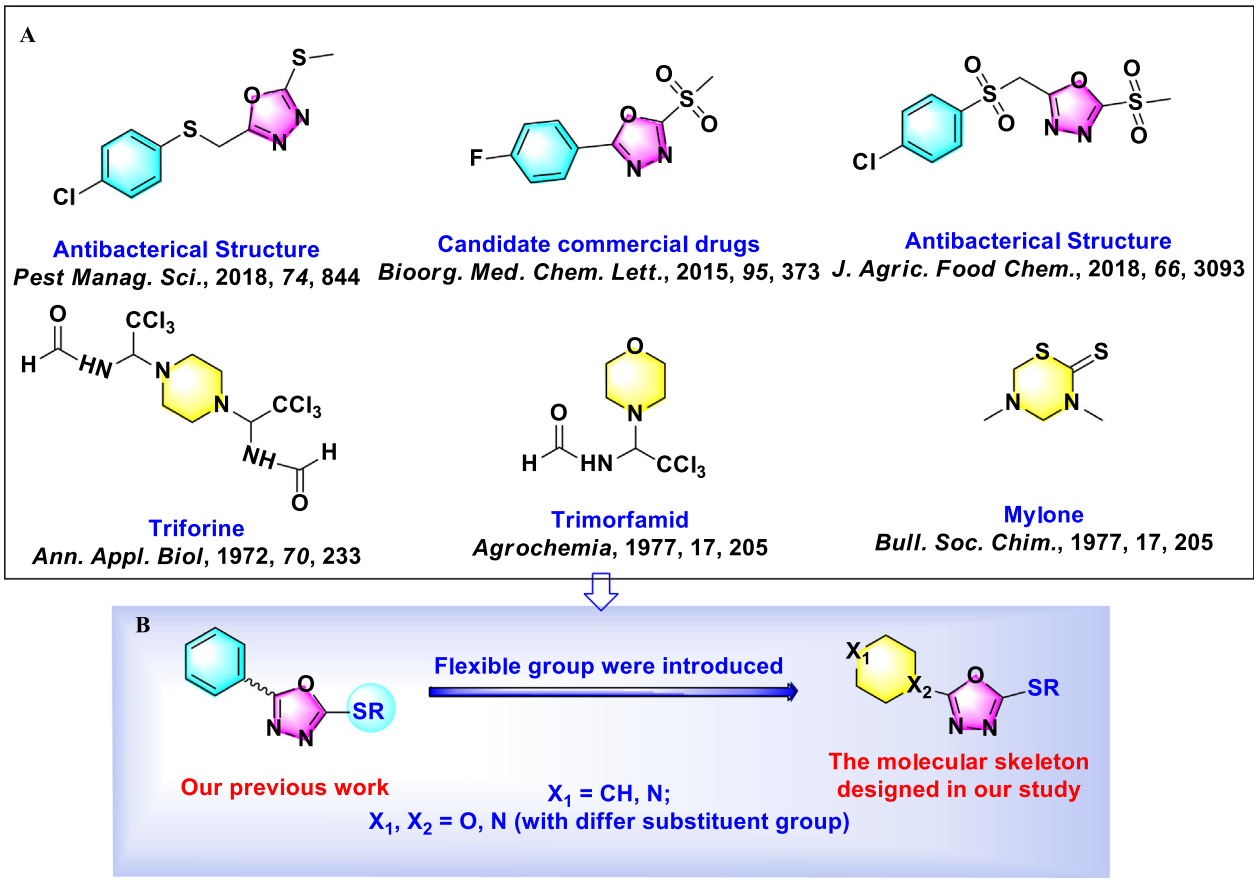

Fig. 1 A) The structures of some bioactive 1,3,4-oxadiazoles thioether derivatives; B) Design concept for the title molecules.

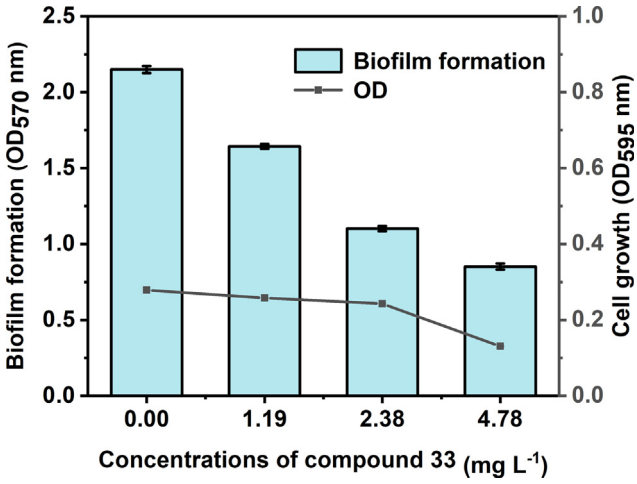

Fig. 2 The effect of molecule **33** on bacterial biofilm by using crystal violet assay.

Thanatephorus cucumeris (*T.c.*), *Sclerotinia sclerotiorum* (*S.s.*), and *Verticillium dahlia* (*V.d.*). Furthermore, pot experiments were conducted under greenhouse conditions to evaluate their control efficiency of the most active target compounds toward rice bacterial blight *in vivo*.

2. Materials and methods

2.1. Instruments and chemicals

The realted NMR data of all title compounds were documented by an JEOL-ECX-500 apparatus (JEOL, Japan). Meanwhile, tetramethylsilane (TMS) served as the internal standard, and $CDCl_3$/DMSO d_6 used as the solvent. Parts per million (ppm) and Hz represents chemical shifts and coupling constants (*J*), respectively. The HRMS data were detected by Thermo Scientific Q Exactive device (UItiMate 3000, Thermo Scientific, The United States). All chemical materials were purchased from commercial market.

2.2. General synthetic process for intermediates and target compounds

*2.2.1. Synthesis of the compound **1***

Raw material 1-methylpiperazine (0.90 g, 8.6 mmol), and TEA (1.75 g, 17.2 mmol), were charged into a 50 mL one-neck round-bottom flask containing 30 mL CH_2Cl_2. After that, this mixture was further stirred for 10 min under ice bath. Phenyl carbonochloridate (1.52 g, 9.4 mmol) was then added dropwise to react at room temperature for 5 h. After the reaction was complete, the mixture was diluted with CH_2Cl_2 and washed with water. The organic layer was further separated and concentrated by vacuum distillation. Finally, desired compound **1** was purified by silica gel chromatography using eluent (CH_2Cl_2: MeOH = 70:1–50:1, V/V).

*2.2.2. Synthesis of the compound **2***

The synthesis of compound **2** was prepared referring with previous literature (Tripathi et al., 2019). In a 25 mL one-neck round-bottom flask, prepared compound **1** (0.50 g, 2.3 mmol) and 3 mL of hydrazine hydrate were added followed by heating at 100 °C for 12 h. Upon completion of the reaction, the mixture was diluted with CH_2Cl_2 and washed with water. The organic layer was separated and concentrated by vacuum distillation. The residue was purified by silica gel chromatography using CH_2Cl_2 and MeOH (50:1–20:1, V/V) as eluent to afford the compound **2**.

*2.2.3. Synthesis of the compound **3***

Compound **3** was synthesized according to previous work (Wang et al., 2019). To a solution of compound **2** (0.37 g, 2.3 mmol), and KOH (0.24 g, 4.4 mmol) in 20 mL of EtOH were added. The resulting mixture was stirred for 10 min, added CS_2 (0.19 g, 2.4 mmol) at 85 °C for another 24 h till almost finished conversion of reation. After reaction completion, the mixture was concentrated, diluted with CH_2Cl_2 and washed with water. The organic layer was separated, concentrated by vacuum distillation, and further purified by silica gel chromatography using CH_2Cl_2 and MeOH (30:1, V/V) as eluent to yield the compound **3**.

*2.2.4. Synthesis of the compound **11***

A 50 mL three-neck round-bottom flask was charged with piperidine-4-carboxylic acid (1.10 g, 8.1 mmol), 2-(isopropyl thio)acetohydrazide (1.36 g, 8.9 mmol) and phosphorus oxychloride (10 mL) were added successively followed by heating at 78 °C for 2.5 h. The excess phosphorus trichloride was removed *in vacuo* and the residue was diluted with ethyl acetate and washed with water. The organic layer was further separated and concentrated by vacuum distillation. The residue was purified by silica gel column chromatography (CH_2Cl_2: MeOH = 10: 1, V/V) to afford compound **11** as a light brown oil 0.69 g, yield 33.66 %.

*2.2.5. Synthesis of the compound **21***

A reaction mixture consisted of tetrahydro-2*H*-pyran-4-carboxylic acid (6.00 g, 44.0 mmol) and 2.5 mL H_2SO_4 in 50 mL CH_3OH. Furthermore, this misture was reacted at 80 °C for 2.5 h. After reaction completion, this mixture was concentrated to removed excess CH_3OH, resulting in yielding desirable residue. Moreover, this residue was further separated by ethyl acetate, washed with water, and purified by silica gel chromatography using eluent (CH_2Cl_2: MeOH = 30:1, V/V) to abtain compound **21** with a white oily liquid.

*2.2.6. Synthesis of the compound **22***

A solution of compound **21** (2.00 g, 14.0 mmol), 3 mL hydrazine hydrate in a 2 mL of CH_3OH was reacted for 20 h, the excess CH_3OH was removed by vacuum distillation and the corresponding residue was extract by ethyl acetate. The organic layer was washed with water, separated and concentrated by vacuum distillation. Finally, the compound **22** was purified by silica gel chromatography using CH_2Cl_2 and MeOH (30:1, V/V) as eluent to achieve white oily liquid.

*2.2.7. Synthesis of the compound **23***

In a 50 mL three-neck round-bottom flask, the compound **22** (0.50 g, 3.30 mmol) and KOH (0.42 g, 6.6 mmol) were added and dissolved in 30 mL EtOH. After the mixture was stirred for 10 min, CS_2 (0.63 mL, 8.2 mmol) was added and then

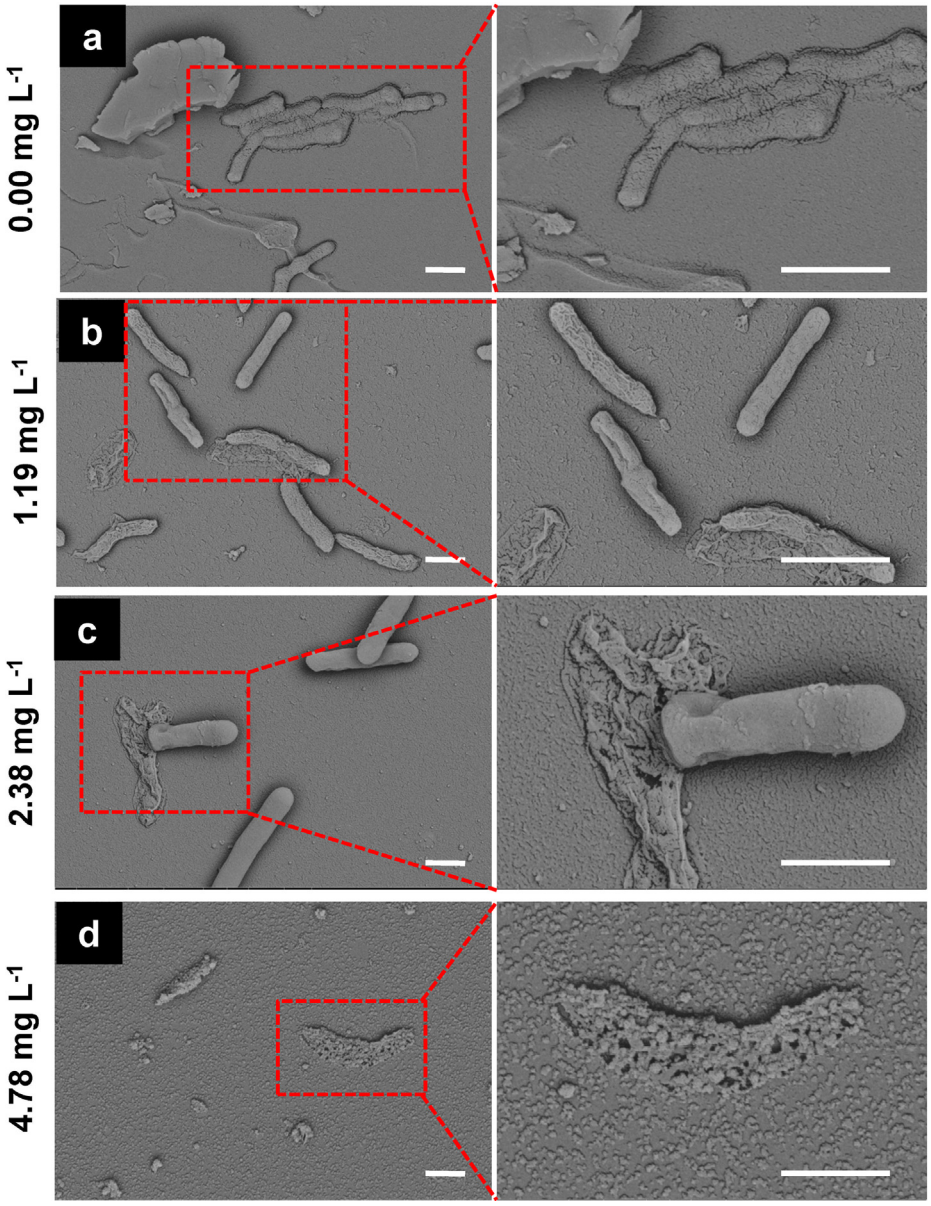

Fig. 3 *Xoo* biofilms formation assay after treatment with compound **33**. Scale bars are 1 μm.

reacted at 85 °C for 1 d. Then, the reaction was quenched by water and extracted by CH_2Cl_2. The organic layer was separated and concentrated by vacuum distillation. The target compound **23** was purified by silica gel chromatography with eluent (CH_2Cl_2: MeOH = 30:1, V/V) to afford an well yield of 49.18 %.

*2.2.8. Synthesis of the title products **4–10***

To achieve desirable target products **4–10**, typical reaction process was carried out. Briefly, appropriate intermediate 3 (0.37 g, 1.8 mmol) and KOH (0.12 g, 2.1 mmol) were added in succession and dissolved in 5 mL DMF, and this mixture was stirred for 10 min. After that, the CH_3I (0.28 g, 1.9 mmol) was added dropwise into this reation and subsequently reacted for 6 h at room temperature. After reaction was complete, this mixture was extracted with ethyl acetate. Finally, desirable target compounds **4–10** were purified by silica gel chromatography using CH_2Cl_2 and MeOH (70:1–40:1, V/V) as eluent to afford the target compounds **4–10**.

*2.2.9. Synthesis of the target compounds **12–20***

A mixture of K_2CO_3 (0.23 g, 1.6 mmol) and compound **11** (0.35 g, 1.4 mmol) in 3 mL of DMF was stirred within 10 min under ice bath, 3-bromoprop-1-yne (0.18 g, 1.5 mmol) was added dropwise and then reacted at 60 °C for 2 d. After the mixture was completed, this mixture poured into water and extracted with ethyl acetate. Furthermore, achieved organic layer was separated, concentrated by vacuum distillation, and further purified by silica gel chromatography using CH_2Cl_2 and MeOH (100:1–50:1, V/V) as eluent to afford corresponding target compounds **12–20**.

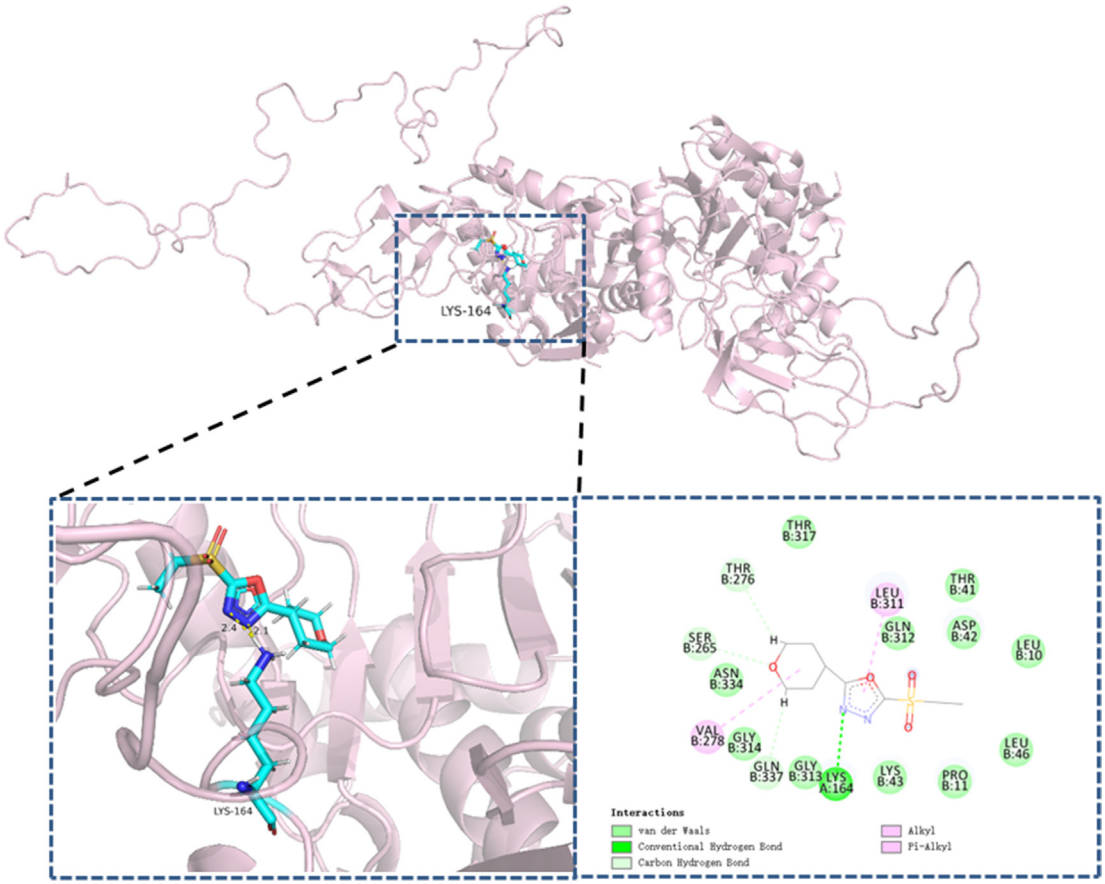

Fig. 4 Docking pose of compound **33** in the possible domain of *Xoo*DLST.

*2.2.10. Synthesis of the target compounds **24–31***

In a solution of compound **23** (0.31 g, 16.0 mmol), and K_2CO_3 (0.24 g, 17.6 mmol) in 10 mL DMF was stirred under ice bath within 10 min. Then, various halogenated hydrocarbon (17.6 mmol) was added dropwise to this mixture for reaction with 6 h. After the completion of the reaction, the mixture was quenched by water and extracted 3 times for ethyl acetate. Finally, the organic layer was combined, concentrated by vacuum distillation, and further purified by silica gel chromatography using a mixture of CH_2Cl_2 and MeOH (70:1–40:1, V/V) to give target compounds **24**–**31**.

*2.2.11. Synthesis of the target compounds **32–34***

The synthesis of target compounds containing sulfone moiety was prepared referring with previous literature (Chen et al., 2019; Li et al., 2018). Briefly, In a mixture of ammonium molybdate (0.12 g, 0.19 mmol) in 30 % hydrogen peroxide was stirred at ice bath for 10 min. Then, the compound **24**–**26** (1.1 mmol) in ethanol (2 mL) were added dropwise and reacted at room temperature for 8 h. After that, the mixture was poured into water and extracted by ethyl acetate. After that, the organic layer was concentrated by vacuum distillation. Moreover, achieved residue was further purified by silica gel chromatography using a mixture of CH_2Cl_2 and MeOH (70:1–40:1, V/V) to successfully yield the target compounds **32**–**34**.

2.3. Experimental section

The methods for antibacterial bioassay *in vitro* and *in vivo* were reported in our previously works (Zhou et al., 2017). The typical mycelium growth rate technique was used for *in vitro* antifungal bioassay from our reported method (Zhou et al., and Zheng et al., 2017, Zeng et al., 2020).

2.4. Plant toxicity test of compound 33 in rice

Rice plant (variety: Xiangliangyou) growth about eight weeks were used in this experiment. Rice leaves were sprayed evenly with 200 mg/L of compound **33** solution or the equivalent DMSO was used as blank control. Then, all the treated rice plants were grown in a plant growth incubator (Light: 28 ℃ for 16 h; Dark:25 ℃ for 8 h) with 90 % RH. Finally, the results were assessed at 14 days after spraying.

2.5. Biofilm inhibition assay

According to literature report (Yang et al., 2016; Zhao et al., 2021), *Xoo* cells were cultured to reach OD_{595} = 0.2 in nutrient broth medium, and further treated with compound **33** to afford final concentrations of 0, 1.19, 2.38 and 4.78 mg/L. The bacteria-containing/without compound solution was

added to sterile 96-well plate and cultured at 28 °C for 72 h in a digital biochemical incubator (Bazargani et al., 2016; Kang et al., 2020). After incubation, the 96-well plates were cleaned with sterile water, and the residual bacterial solution was removed and dried at 37 °C. Fixed with Carnot's fixative solution for 30 min, then washed with sterile H_2O. The dried samples were treated with 1 % crystal violet The dried samples were stained with 1 % crystal violet for 30 min. After that, these samples were further cleaned with H_2O. Finally, 95 % ethanol was used to dissolve the previously stained sample. OD_{570} was determined with a microplate reader to evaluate the quantification of biofilm formation.

2.6. Biofilm imaging assay

Biofilm study was carried out according to previous work (Milling et al., 2011, Zhou et al., 2019; Kakkar et al., 2015). *Xoo* cells were cultivated to OD_{595} = 0.1, transferred to six-well polystyrene plates and then covered with round glass. After 5 days of treatment with compound **33** at different dosages (0, 1.19 mg/L, 2.38 mg/L, or 4.78 mg/L), *Xoo* cells were rinsed gently with phosphate-buffered saline media, and these samples were further post-fixed in situ in 2.5 % glutaraldehyde solution. After that, these samples were then gradually dehydrated with increasingly concentrated ethanol. At last, these samples were observed with scanning electron microscopy (SEM) after undergoing steps such as freeze-drying and gold plating.

2.7. Molecule docking

For the docking study, according to previous work (Zhu et al., 2022), the three-dimensional model of *Xoo*DLST was obtained by using Swiss-Model: the protein sequence of *Xoo*DLST was A0A0K0GL90, which achieved in Uniprot, and the template of DLST (PDB code:7b9k.1.A) was used. Then, the theoretical model of *Xoo*DLST was further assessed, and result was provided in Support Information. Finally, docking outcomes were achieved by Sybyl X 2.0, and further displayed by Discovery Studio 2020 and PyMol software. Docking accuracy was certified as root-mean-square deviation (RMSD) by Sybyl X 2.0 software.

3. Results and discussion

3.1. Synthesis of target compounds 4–10, 12–20 and 24–34.

The synthetic routes of target compounds **4**–**10**, **12**–**20**, and **24**–**34** were displayed in Schemes 1–3, respectively. Three series of 1,3,4-oxadiazole thioether derivatives with a thioether group at the 5-position and a piperazine/piperidine/morpholine moiety at the 2-position were synthesized, and three 1,3,4-oxadiazole sulfone derivatives were successfully constructed with a morpholine ring at the 2-position. Analysis of the structure–activity relationships in these compounds was limited owing to the long synthetic route, complex raw materials, and different synthetic conditions. First, using 1-methylpiperazine as the starting material, compound **3** was prepared in a three-step sequence, comprising acylation, hydrazinolysis, and cyclization, then derivatized with differently substituted halogenated compounds to obtain target compounds **4**–**10** in moderate yields. Second, 1-methylpiperidine-4-carboxylic acid and 2-(isopropylthio) acetic acid were reacted using phosphorus oxychloride as solvent at 78 °C to obtain compound **11**, and a subsequent substitution reaction in DMF proceeded promptly to afford target compounds **12**–**20** in higher yields. Finally, tetrahydro-2*H*-pyran-4-carboxylic acid was used as raw material to yield compound **22** by undergoing substitution and acylation steps, then ring-closed with CS_2 and derivatized with differently substituted halogenated compounds to obtain target compounds **24**–**31**. Sulfone compounds **32**–**34** were then prepared by oxidation of **24**–**26**, respectively, using H_2O_2 as oxidant and ammonium molybdate as catalyst (referenced by Li et al., 2018; Chen et al., 2019). These title compounds were confirmed by NMR and HRMS (Corresponding data could be shown in the supporting information Figure S1-Figure S91).

3.2. In vitro bioassay results of compounds 4–10, 12–20, and 24–34.

The *in vitro* bioassay results of the synthesized title compounds towards *Xoo*, *Xac*, and *Psa* were assayed by introducing turbidimetric method, with positive controls pesticides [commer-

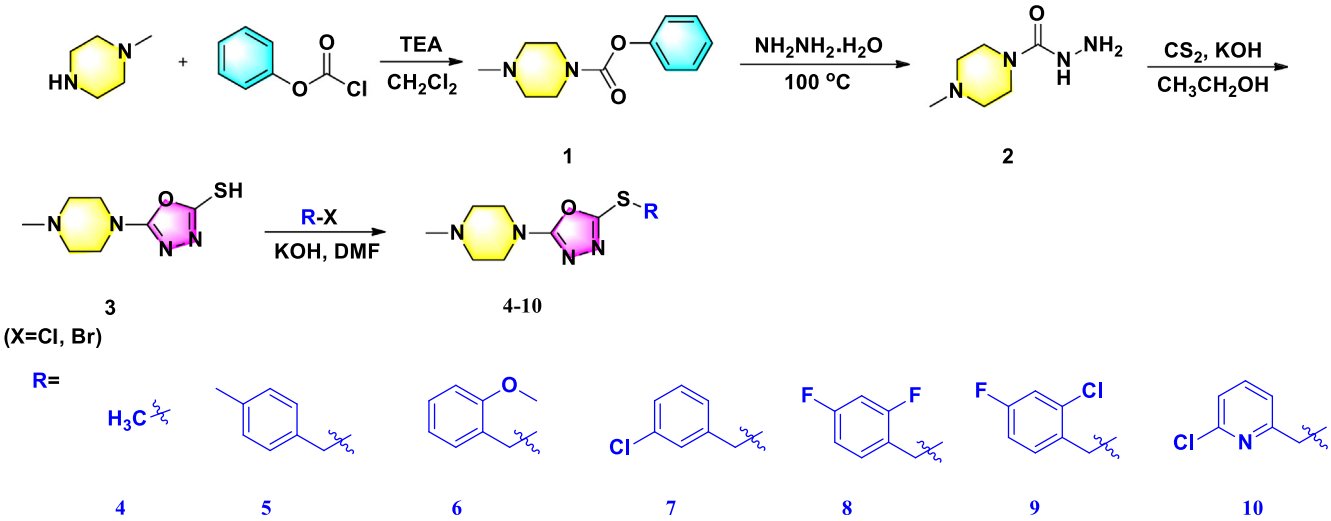

Scheme 1 Synthetic route for the title molecules 4–10.

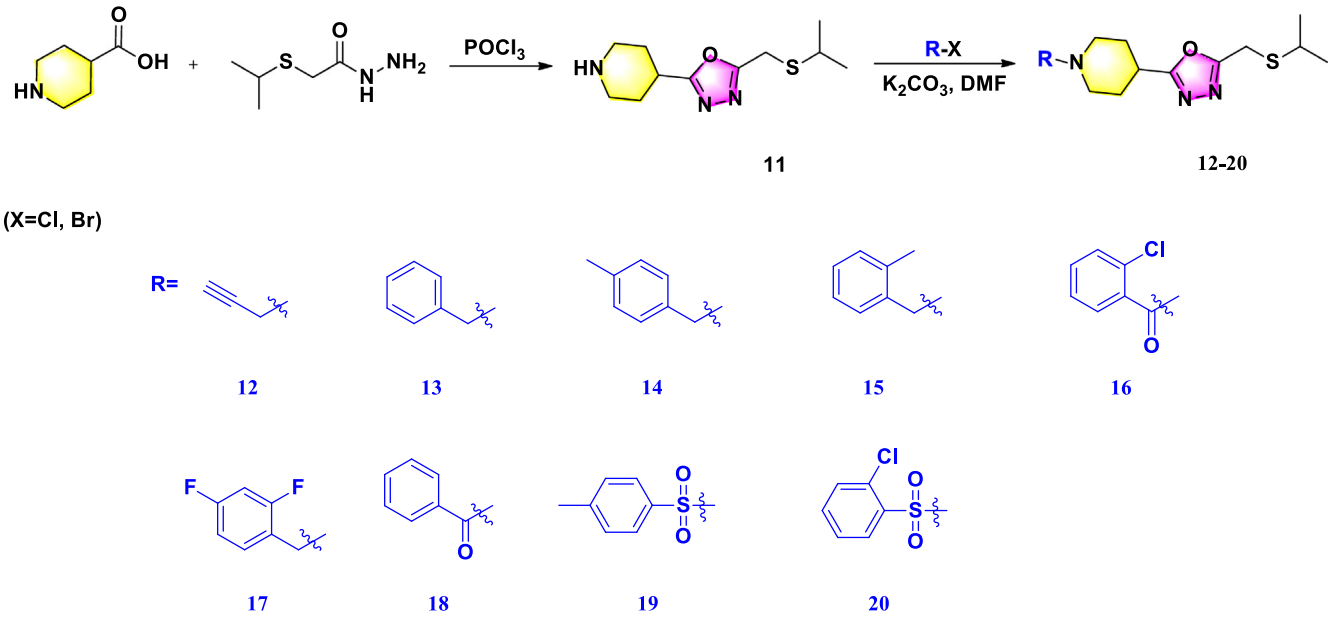

Scheme 2 Synthetic route for the title molecules 12–20.

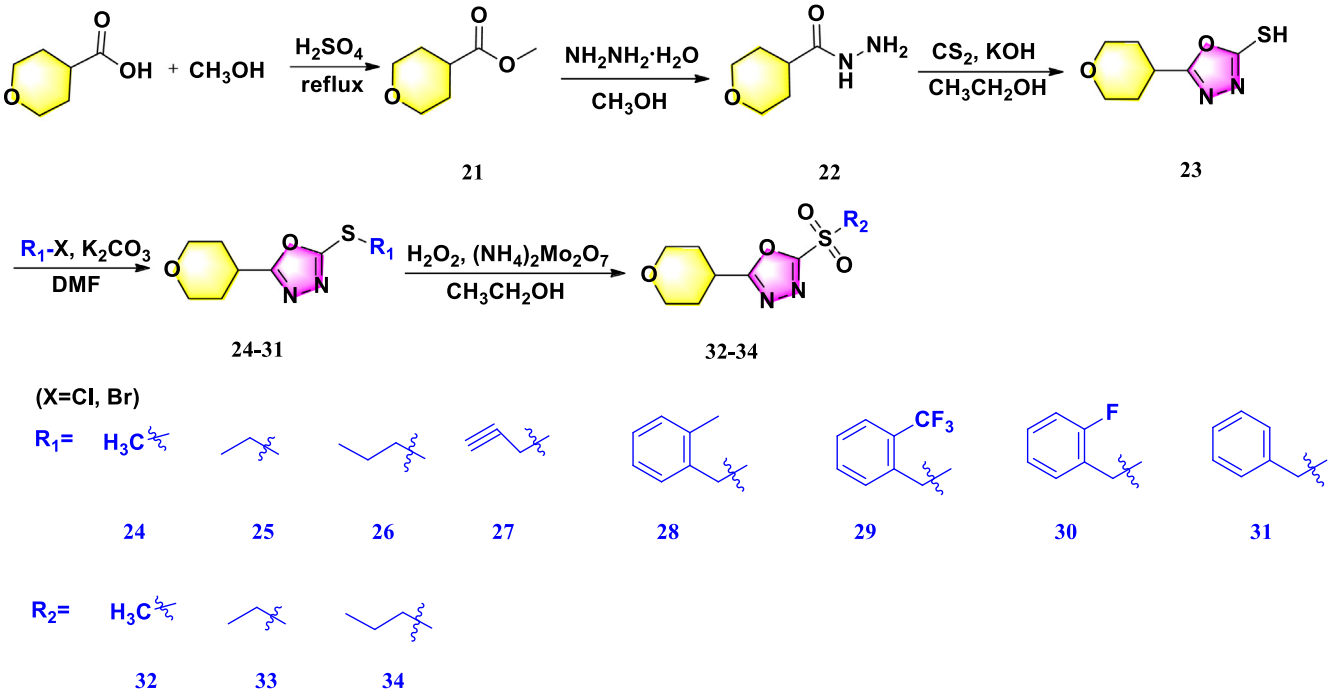

Scheme 3 Synthetic route for the title molecules 24–34.

cialized bismerthiazol (**BT**) and thiodiazole copper (**TC**)]. Notably, the preliminary screening results (Table 1) suggested that most of the designed 1,3,4-oxadiazole thioether derivatives possessed weak antibacterial ability, with only **5**, **14**, **15**, and **16** exhibiting an inhibition activity of > 50 % at 100 mg L^{-1}. In addition, thioether compounds substituted with a piperidine structure at 100 mg L^{-1}, such as **14**, **15**, and **16**, showed good anti-*Xac* ability, with inhibition rates of 56.46 %, 55.62 %, and 86.96 %, respectively. Pleasingly, the anti-*Xoo* ability was greatly improved when thioether derivatives (**24**–**26**) were oxidized to sulfone derivatives (**32**–**34**). The designed sulfone derivatives showed distinct selectivity for the tested bacterial strain and excellent bioactivity against *Xoo*, with inhibition rates of > 95 % at both 100 and 50 mg L^{-1}. However, they possessed poor antibacterial ability against *Xac* and *Psa*, with inhibition rates of < 50 % at 100 mg L^{-1}. Furthermore, EC_{50} values of the partially active compounds against *Xoo* were further evaluated, with the

Table 1 Antibacterial activity of compounds **4**–**10**, **12**–**20**, and **23**–**34** against *Xoo*, *Xac*, and *Psa in vitro*.

Compounds	*Xoo*		*Xac*		*Psa*	
	100 mg/L	**50** mg/L	**100** mg/L	**50** mg/L	**100** mg/L	**50** mg/L
4	0	0	0	0	0	0
5	18.53 ± 1.51	0	73.83 ± 1.03	40.74 ± 8.25	48.35 ± 6.23	34.88 ± 5.68
6	0	0	36.22 ± 4.11	25.79 ± 6.78	34.80 ± 2.98	28.91 ± 2.17
7	55.24 ± 0.99	32.11 ± 0.57	31.11 ± 9.90	0	59.70 ± 1.46	33.74 ± 0.66
8	58.58 ± 1.06	15.78 ± 1.44	0	0	0	0
9	34.75 ± 1.08	0	0	0	37.83 ± 2.72	19.41 ± 2.20
10	44.89 ± 0.69	28.79 ± 3.65	0	0	40.05 ± 2.31	10.88 ± 1.79
12	33.83 ± 1.05	27.03 ± 1.49	35.24 ± 5.05	22.74 ± 5.52	14.34 ± 1.78	0
13	16.42 ± 2.29	10.85 ± 1.29	43.83 ± 3.11	33.15 ± 6.26	0	0
14	41.47 ± 2.48	25.91 ± 3.69	56.46 ± 1.75	41.02 ± 3.63	0	0
15	16.37 ± 7.48	0	55.62 ± 5.74	39.19 ± 5.97	0	0
16	48.74 ± 2.40	0	86.96 ± 0.67	68.38 ± 1.72	16.29 ± 1.69	0
17	21.80 ± 1.54	15.23 ± 1.63	18.20 ± 4.61	0	0	0
18	0	0	16.04 ± 1.76	0	13.29 ± 2.1	0
19	0	0	19.09 ± 1.57	0	0	0
20	32.08 ± 4.20	23.38 ± 3.56	37.91 ± 6.79	0	0	0
23	100	96.72 ± 4.47	35.43 ± 5.64	0	28.59 ± 0.64	23.28 ± 1.83
24	40.31 ± 4.42	16.71 ± 0.55	15.57 ± 3.02	0	16.72 ± 3.37	10.96 ± 2.57
25	36.68 ± 4.19	19.29 ± 0.39	0	0	0	0
26	39.25 ± 1.03	0	0	0	0	0
27	49.47 ± 5.24	15.67 ± 4.78	41.24 ± 1.09	16.02 ± 2.69	39.44 ± 0.76	26.27 ± 3.55
28	31.67 ± 3.62	12.23 ± 1.72	32.05 ± 2.56	22.57 ± 2.44	24.24 ± 6.75	15.82 ± 1.13
29	24.66 ± 3.49	0	0	0	0	0
30	15.82 ± 1.82	10.62 ± 0.47	0	0	0	0
31	20.97 ± 1.31	10.26 ± 1.92	0	0	0	0
32	100	100	49.52 ± 2.01	37.20 ± 1.94	29.98 ± 1.69	0
33	100	99.19 ± 0.70	41.36 ± 3.01	0	0	0
34	100	97.24 ± 2.13	45.78 ± 1.98	16.59 ± 1.38	31.98 ± 2.01	11.09 ± 1.79
BT	100	53.90 ± 0.39	42.8 ± 0.58	24.70 ± 0.58	27.90 ± 0.17	10.50 ± 0.48
TC	40.1 ± 0.19	26.30 ± 0.38	34.8 ± 0.39	18.90 ± 0.78	15.20 ± 0.15	0

results (Table 2) showing that compounds **32**–**34** displayed excellent anti-*Xoo* activity, with corresponding EC_{50} values of 5.18, 1.20, and 8.26 mg L^{-1}, respectively, which were much surpass to commercialized **BT** (35.04 mg L^{-1}) and **TC** (> 100 mg L^{-1}). These outcomes displayed that the integration of two bioactive components can facilitate the discovery of highly effective, biologically active alternatives.

3.3. Antifungal activity

Furthermore, the most recognized mycelium growth rate method was carried out to achieve their antifungal properties toward *G. zeae*, *F. oxysporum*, *B. dothidea*, *S. sclerotiorum*, *V. dahlia*, and *T. cucumeris*. Commercial agents fluopyram (**FP**) and boscalid (**BS**) served as positive controls pesticides. As shown in Table 3, all thioether derivatives displayed no activity against the tested fungi, with only sulfone derivative **32** showing relatively good fungicidal activity, with inhibition rates of 53.83 %, 45.64 %, 51.32 %, 98.86 %, 99.42 %, and 52.13 %, respectively. Furthermore, the EC_{50} values of compound **32** against *S. sclerotiorum* and *V. dahlia* were measured as 22.16 and 32.78 mg L^{-1}, respectively. SAR analysis showed that the fungicidal ability was not present when a piperazine/piperidine/morpholine ring was introduced at the 2-position and different sulfur moieties were introduced at the 5-position of the 1,3,4-oxadiazole ring. Furthermore, the potency was significantly improved when thioether derivatives were oxidized to sulfone derivatives. For example, the fungicidal activities of sulfone derivatives **32**–**34** were much better than those of corresponding thioether derivatives **24**–**26**, respectively. Furthermore, introducing a methyl group (compound **32**) onto the sulfone moiety resulted in more broad fungicidal potency compared with introducing a multi-carbon group (compounds **33** and **34**). This outcome indicated that an increasing chain length hampered the antifungal ability of the designed sulfone compounds (see Tables 3 and 4).

Table 2 Assessment of EC_{50} values of compounds **23**, **32**, **33**, and **34** toward *Xoo in vitro*.

compounds	*Xoo*		
	Regression equation	R^2	EC_{50} (mg L^{-1})
23	y = 6.544x-2.467	0.985	13.84 ± 1.17
32	y = 4.158x + 2.030	0.992	5.18 ± 0.30
33	y = 3.892x + 4.698	0.999	1.20 ± 0.09
34	y = 3.873x + 1.447	0.975	8.26 ± 0.68
BT	y = 4.182x-1.459	0.919	35.04 ± 0.77
TC	y = 3.405x-1.821	0.994	100.6 ± 0.89

3.4. Effects of various dosage of compound 33 on biofilm

Bacterial biofilm is a crucial virulence factor for phytopathogenic bacteria, and provides crucial physical barriers

Table 3 The *in vitro* antifungal properties of title compounds **4**–**10**, **12**–**20**, and **23**–**34** at 100 mg/L towards six plant fungal strains.

Compounds	*G.z.*	*F.o.*	*B.d.*	*S.s.*	*V.d.*	*T.c.*
	100 mg/L	100 mg/L	100 mg/L	100 mg/L	100 mg/L	100 mg/L
4	0	0	0	0	0	0
5	0	0	0	0	0	0
6	0	0	0	0	0	0
7	0	0	0	0	0	0
8	0	0	0	0	0	0
9	0	0	0	0	0	0
10	0	0	0	0	0	0
12	0	0	0	0	0	0
13	0	0	0	0	0	0
14	0	0	0	0	0	0
15	0	0	0	0	0	0
16	0	0	0	0	0	0
17	0	0	0	0	0	0
18	0	0	0	0	0	0
19	0	0	0	0	0	0
20	0	0	0	0	0	0
23	0	0	0	0	0	0
24	0	0	0	0	0	0
25	0	0	0	0	0	0
26	0	0	0	0	0	0
27	0	0	0	0	0	0
28	0	0	15.73 ± 1.65	0	15.42 ± 1.94	0
29	0	0	0	0	0	0
30	0	0	0	0	0	0
31	0	0	0	0	0	0
32	53.83 ± 1.94	45.64 ± 1.46	51.32 ± 1.41	98.86 ± 1.08	99.42 ± 1.17	52.13 ± 1.94
33	11.33 ± 1.88	0	0	49.04 ± 1.87	16.03 ± 1.15	0
34	35.87 ± 1.99	30.15 ± 1.17	54.32 ± 1.73	24.85 ± 1.07	29.43 ± 2.64	60.13 ± 3.05
BS	98.23 ± 1.95	88.44 ± 2.27	91.59 ± 2.17	60.01 ± 1.17		
FP	100	90.38 ± 1.1	57.59 ± 11.19	85.01 ± 2.06		

to delay of plant defense responses as well as reduce bactericidal potency. Therefore, to further confirm the inhibitory potency of compound **33** on biofilm, biofilm experiments were carried out, and evaluated using crystal violet staining. The measured optical density value (OD_{570}) of compound **33** on biofilms is displayed in Fig. 2. In the absence of compound **33** (control sample), the amount of biofilm formation was largest (2.15), and decreased with an increasing concentration of **33**. Biofilm formation was clearly decreased by 12.7 %, 21.3 %, and 30.4 % after cotreatment with compound **33** at various concentrations (1.19, 2.38, and 4.78 mg L^{-1}, respectively).

3.5. Biofilm formation imaging assay through using scanning electron microscopy (SEM)

To further verify the biofilm disruption effects of compound **33**, SEM was conducted to visualize the bacterial biofilm formation of *Xoo*. As shown in Fig. 3, unbroken intact biofilms and *Xoo* were observed in control samples. Meanwhile, in the absence of compound **33**, *Xoo* cells were tightly covered in the extracellular matrix. However, after treatment of *Xoo* cells with compound **33**, a broken extracellular matrix was observed, and numerous *Xoo* cells emerged on the biofilm surface. At a compound dosage of 2.38 mg L^{-1}, part of the cell biofilm was completely destroyed and some cells had died. More interestingly, when the dosage was upgraded to 4.78 mg L^{-1}, all cells were dead. Above-mentioned results showed that treatment with compound **33** (1.19–4.78 mg L^{-1}) inhibited not only the *Xoo* cell membrane, but also the formation of a large number of biofilms, and thereby further inhibiting bacterial virulence factors.

3.6. Molecular docking

To account for the most profiling compound **33** against phytopathogen, molecular docking was conducted to investigate their possible interactions with the *Xoo*DLST. The theoretical model of *Xoo*DLST from section 2.6 was utilized in all docking simulations. As displayed in Fig. 4, the core scaffold of compound **33** was engaged in the binding pocket of *Xoo*DLST through interaction with Lys 164 residue. In particular, we found that N atom on 1,3,4-oxadiazole ring of compound **33** could interact with amino group of Lys 164 residue via hydrogen bonding, the O atom on 1,3,4-oxadiazole ring of compound **33** interacts with other residues through alkyl, and van der Waals interaction. More interestingly, lysine was found, and certified as the crucial amino acid for succinylation modification. Suggesting that compound **33** might inhibit the succinylation modification of Lys 164 residue, and thereby resulting in disrupting the function of DLST.

Table 4 Assessment of EC_{50} values of compound **32** against *S. sclerotiorum* and *V. dahlia in vitro*.

Compounds	Pathogens	Regression equation	EC_{50} (mg L^{-1})
32	*S.s.*	y = 2.289x + 1.919	22.17 ± 0.73
32	*V.d.*	y = 4.659x-2.062	32.78 ± 0.70
BS	*S.s.*	y = 8.725x-11.712	82.28 ± 2.14
FP	*S.s.*	y = 2.357x + 1.287	37.56 ± 1.57

In general, binding modes was called "well-docked", that the RMSD value was < 2.0 Å with respect to the minimized reference structure. Both the "turned" and "nonturned" compound **33**'s poses were used for evaluating the RMSD value. The parameters (Similarity: 9.461; RMSD: 0.427) were provided by Sybyl X 2.0 software. Thus, the results declared that the predicted poses seem reasonable due to the RMSD of 0.427 was lower than 2.0.

Above-mentioned outcomes indicated that the morpholine ring was favor to target the *Xoo*DLST to a certain extent.

*3.7. The control efficiency of compound **33** toward rice bacterial leaf blight*

To achieve a potential control efficiency for managing plant bacterial diseases, compound **33** was selected based on its superior bioactivity (anti-*Xoo* potency, EC_{50} = 1.19 mg L^{-1}) to evaluate the control efficiency toward rice bacterial leaf blight. As displayed in Table 5, compound **33** exhibited good activity toward rice bacterial leaf blight, providing corresponding acceptable curative (53.63 %) and good protective activities (50.00 %) at 200 mg L^{-1}. These were slightly superior than commercial **BT** (curative activity: 39.09 %; protective activity: 38.18 %) and **TC** (curative activity: 39.54 %; protective activity: 37.27 %), respectively. Furthermore, 0.1 % of orange peel essential oil (OPO) and organic silicon (SI) were used as auxiliaries, which are expected to enhance the physical and chem-

Table 5 The control efficiency of compound **33** toward rice bacterial blight at 200 mg/L *in vivo*.

Treatment	Protective activity (14 days after spraying)			Curative activity (14 days after spraying)		
	Morbidity (%)	Disease index (%)	Control efficiency (%)	Morbidity (%)	Disease index (%)	Control efficiency (%)
33	100	40.74	50.00	100	37.77	53.63
33-SI	100	38.27	53.03	100	29.91	60.66
33-OPO	100	36.29	55.45	100	31.48	61.36
BT	100	50.37	38.18	100	49.62	39.09
TC	100	51.11	37.27	100	49.25	39.54
CK	100	81.48		100	81.48	

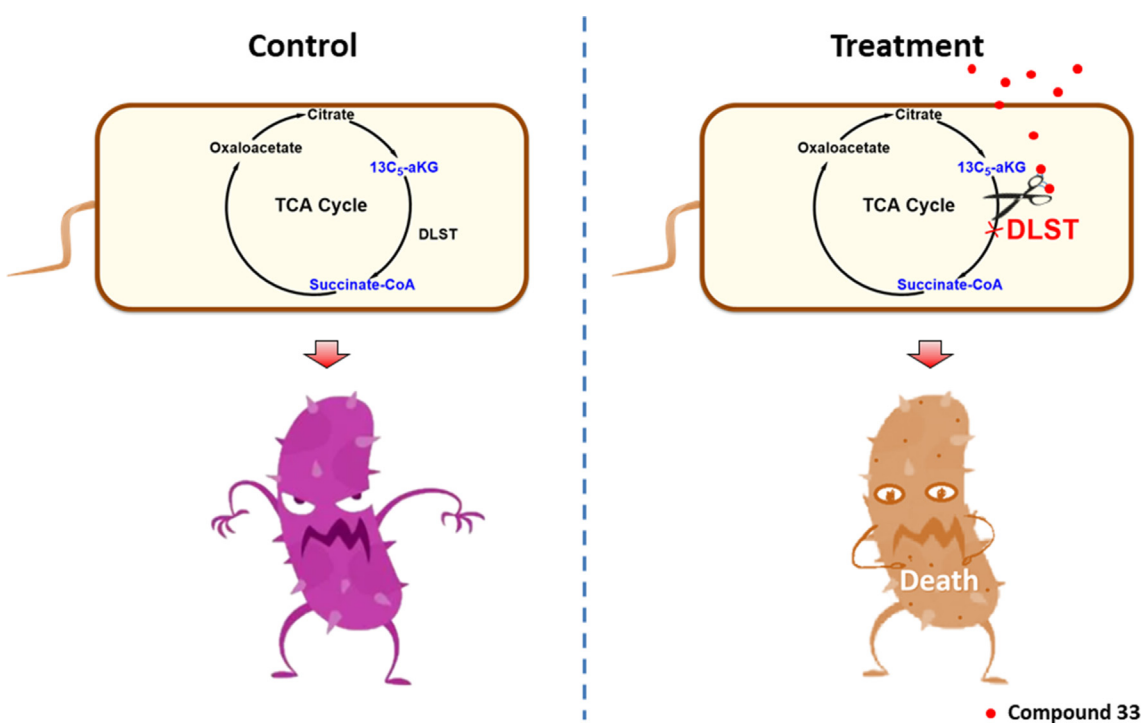

Fig. 5 Hypothetical model of compound **33** inhibiting DLST function of *Xoo* and resulting in disruption of *Xoo*'s invasion process.

ical properties of the compound, to obtain better potency. Therefore, pot experiments were conducted concurrently, with the addition of auxiliaries shown to significantly enhance the control efficacy of compound **33** (200 mg L^{-1}) toward rice bacterial blight. Improved curative and protective activities of 60.66 % and 53.03 % (organic silicon), and 61.36 % and 55.45 % (orange oil), respectively, were obtained, which were superior to these of compound **33** alone.

*3.8. Phytotoxicity of compound **33** at 200 mg L^{-1} toward rice plants after seven days under greenhouse conditions*

To further verify the safety of our designed compounds toward plants, the most bioactive compound against *Xoo*, **33**, was selected and assessed for its phytotoxicity toward rice plants, and providing an equivalent amount of DMSO used as the blank control. The results showed no adverse impact on the rice leaf and haulm at 7 days after treatment with compound **33** at 200 mg L^{-1} (**Figure S92**), which proved that compound **33** was safe toward rice. All experiments suggested that the designed molecular skeleton showed potential application prospects as an antibacterial agent in agriculture.

4. Conclusions

An array of 1,3,4-oxadiazole thioether/sulfone derivatives bearing a piperazine/piperidine/morpholine group were elaborately prepared, and their antibacterial potency toward three phytopathogenic bacteria and six phytopathogenic fungi were systematically evaluated. The preliminary antibacterial screening outcomes showed that these compounds possessed broad-spectrum bioactivities toward the tested bacterial strains. Compounds **32** and **33** showed significant antibacterial potency toward *Xoo*, with EC_{50} values of 5.17 and 1.19 mg L^{-1}, respectively, which were surpass to commercialized **BT** and **TC**. Pot experiments indicated that 200 mg L^{-1} of compound **33** exhibited good efficiency toward rice bacterial blight, with acceptable curative efficiency (53.63 %) and protective efficiency (42.72 %), which were slightly better than commercialized **BT** (39.09 % and 38.18 %) and **TC** (39.54 % and 37.27 %). Interestingly, adding organic silicon or orange peel essential oil as 0.1 % auxiliaries significantly enhanced the control efficacy of compound **33** toward rice bacterial blight, resulting in improved curative and protective activities of 53.03 % and 63.28 % (organic silicon), and 55.45 % and 61.36 % (orange peel essential oil), respectively. Meanwhile, compound **33** showed low phytotoxicity toward rice plants at 200 mg L^{-1}. Furthermore, antifungal bioassay outcomes demonstrated that newly designed 1,3,4-oxadiazole sulfone derivative **32** exhibited broad-spectrum activity against the tested fungi, especially *S. sclerotiorum* and *V. dahlia*, providing EC_{50} values of 22.16 and 32.78 mg L^{-1}, respectively. Furthermore, a hypothetical model (Fig. 5) of compound C_{11} targeting DLST was proposed by using SEM, biofilm assay, and molecular docking study. Considering these merits of title compounds (e.g., simple molecular frameworks and significant bioactivities), these types of sulfone compound can be served as promising antimicrobial alternatives through targeting DLST, and further structural modification is underway in our laboratory.

CRediT authorship contribution statement

Fang Wang: Writing – original draft, Data curation. **Bin-Xin Yang:** Data curation. **Tai-Hong Zhang:** Formal analysis. **Qing-Qing Tao:** Data curation. **Xiang Zhou:** Data curation, Resources, Writing – review & editing. **Pei-Yi Wang:** Methodology. **Song Yang:** Conceptualization, Funding acquisition, Project administration, Resources, Validation, Writing – review & editing.

Declaration of Competing Interest

The authors declare no competing financial interest.

Acknowledgments

We acknowledge the supports from National Natural Science Foundation of China (21877021, 32160661), the Guizhou Provincial S&T Project (2018[4007]), the Guizhou Province [Qianjiaohe KY number (2020)004]), Program of Introducing Talents of Discipline to Universities of China (D20023, 111 Program) and GZU (Guizhou University) Found for Newly Enrolled Talent (No. 202229). The authors thank Simon Partridge (PhD) for supervising the draft of this manuscript.

Appendix A. Supplementary material

Supporting information including ^{1}H NMR, ^{13}C NMR, ^{19}F NMR and HRMS spectra associated with this article can be found.

Supplementary data to this article can be found online at https://doi.org/10.1016/j.arabjc.2022.104479.

References

Bauske, M.J., Mallik, I., Yellareddygari, S.K.R., Gudmestad, N.C., 2018. Spatial and temporal distribution of mutations conferring QoI and SDHI Resistance in *Alternaria solani* across the united states. Plant Dis. 102 (2), 349–358. https://doi.org/10.1094/PDIS-06-17-0852-RE.

Bazargani, M.M., Rohloff, J., 2016. Antibiofilm activity of essential oils and plant extracts against *Staphylococcus aureus* and *Escherichia coli* biofilms. Food Control. 61, 156–164. https://doi.org/10.1016/j.foodcont.2015.09.036.

Benedik, J.M., Gibbs, P.R., Riddle, R.R., 1998. Microbial denitrogenation of fossil fuels. Trends Biotechnol. 16 (9), 390–395. https://doi.org/10.1016/S0167-7799(98)01237-2.

Chen, B., Long, Q.S., Zhao, Y.L., Wu, Y.Y., Ge, S.S., Wang, P.Y., Yang, C.G., Chi, Y.G., Song, B.A., Yang, S., 2019b. Sulfone-based probes unraveled dihydrolipoamide *S*-succinyltransferase as an unprecedented target in phytopathogens. J. Agr. Food Chem. 67 (25), 6962–6969. https://doi.org/10.1021/acs.jafc.9b02059.

Chen, B., Long, Q.S., Meng, J., Zhou, X., Wu, Z.B., Tuo, X.X., Ding, Y., Zhang, L., Wang, P.Y., Li, Z., Yang, S., 2020b. Target discovery in *Ralstonia solanacearum* through an activity-based protein profiling technique based on bioactive oxadiazole sulfones. J. Agr. Food Chem. 68 (8), 2340–2346. https://doi.org/10.1021/acs.jafc.9b07192.

Chen, J.X., Yi, C.F., Wang, S.W., Wu, S.K., Li, S.Y., Hu, D.Y., Song, B.A., 2019a. Novel amide derivatives containing 1,3,4-thiadiazole moiety: Design, synthesis, nematocidal and antibacterial activities. Bioorg. Med. Chem. Lett. 29 (10), 1203–1210. https://doi.org/10.1016/j.bmcl.2019.03.017.

Chen, J.X., Luo, Y.Q., Wei, C.Q., Wu, S.K., Wu, R., Wang, S.B., Hu, D.Y., Song, B.A., 2020a. Novel sulfone derivatives containing a 1,3,4-oxadiazole moiety: design and synthesis based on the 3D-QSAR model as potential antibacterial agent. Pest Manag. Sci. 76 (9), 3188–3198. https://doi.org/10.1002/ps.5873.

Fisher, M.C., Hawkins, N.J., Sanglard, D., Gurr, S.J., 2018. Worldwide emergence of resistance to antifungal drugs challenges human

health and food security. Science 360 (6390), 739–742. https://doi.org/10.1126/science.aap7999.

Formagio, A.S.N., Tonin, L.T.D., Foglio, M.A., Madjarof, C., Carvlho, J.E.D., Costa, W.F.D., Cardoso, F.P., Sarragiotto, M. H., 2008. Synthesis and antitumoral activity of novel 3-(2-substituted-1,3,4-oxadiazol-5-yl) and 3-(5-substituted-1,2,4-triazol-3-yl) β-carboline derivatives. Bioorg. Med. Chem. 16 (22), 9660–9667. https://doi.org/10.1016/j.bmc.2008.10.008.

Gan, X.H., Hu, D.Y., Chen, Z., Wang, Y.J., Song, B.A., 2017. Synthesis and antiviral evaluation of novel 1,3,4-oxadiazole/thiadiazole-chalcone conjugates. Bioorg. Med. Chem. Lett. 27 (18), 4298–4301. https://doi.org/10.1016/j.bmcl.2017.08.038.

Gould, F., Brown, Z.S., Kuzma, J., 2018. "Wicked evolution: Can we address the sociobiological dilemma of pesticide resistance. Science 360 (6390), 728–732. https://doi.org/10.1126/science.aar3780.

Guo, S.X., He, F., Song, B.A., Wu, J., 2021. Future Direction of agrochemical development for plant disease in china. Food Energy Secur. 10 (4), e293.

Huang, J., Bushey, D.F., 1987. Novel 1,3,4-oxadiazol-2(3*H*)-ones as potential pest control agents. J. Agr. Food Chem. 35 (3), 368–373. https://doi.org/10.1021/jf00075a022.

Kakkar, A., Nizampatnam, N.R., Kondreddy, A., Pradhan, B.B., Chatterjee, S., 2015. *Xanthomonas campestris* cell-cell signalling molecule DSF (diffusible signal factor) elicits innate immunity in plants and is suppressed by the exopolysaccharide xanthan. J. Exp. Bot. 66 (21), 6697–6714. https://doi.org/10.1093/jxb/erv377.

Kang, J.M., Liu, L., Liu, Y.F., Wang, X.Y., 2020. Ferulic acid inactivates *Shigella flexneri* through cell membrane destructieon, biofilm retardation, and altered gene expression. J. Agr. Food Chem. 68 (27), 7121–7131. https://doi.org/10.1021/acs.jafc.0c01901.

Li, P., Yin, J., Xu, W.M., Wu, J., He, M., Hu, D.Y., Yang, S., Song, B. A., 2013. Synthesis, antibacterial activities, and 3D-QSAR of sulfone derivatives containing 1,3,4-oxadiazole moiety. Chem. Biol. Drug Des. 82 (5), 546–556. https://doi.org/10.1111/cbdd.12181.

Li, P., Hu, D.Y., Xie, D.D., Chen, J.X., Jin, L.H., Song, B.A., 2018. Design, synthesis, and evaluation of new sulfone derivatives containing a 1,3,4-oxadiazole moiety as active antibacterial agents. J. Agri. Food Chem. 66 (12), 3093–3100. https://doi.org/10.1021/acs.jafc.7b06061.

Lu, W., Pan, L., Zhao, H., Jia, Y., Wang, Y., Yu, X., Wang, X., 2014. Molecular detection of *Xanthomonas oryzae* pv. *oryzae*, *Xanthomonas oryzae* pv. *oryzicola*, and *Burkholderia glumae* in infected rice seeds and leaves. Crop. J. 2 (6), 398–406. https://doi.org/10.1016/j.cj.2014.06.005.

Milling, A., Babujee, L., Allen, C., 2011. *Ralstonia solanacearum* extracellular polysaccharide is a specific elicitor of defense responses in wilt-resistant tomato plants. PLoS One 6 (1), e15853.

Savary, S., Willocquet, L., Pethybridge, S.J., Esker, P., McRoberts, N., Nelson, A., 2019. The global burden of pathogens and pests on major food crops. Nat. Ecol. Evol. 3 (3), 430–4439. https://doi.org/10.1038/s41559-018-0793-y.

Su, S.H., Zhou, X., Liao, G.P., Qi, P.Y., Jin, L.H., 2016. Synthesis and antibacterial evaluation of new sulfone derivatives containing 2-aroxymethyl-1,3,4-oxadiazole/thiadiazole moiety. Molecules 22 (1), 64. https://doi.org/10.3390/molecules22010064.

Tao, Q.Q., Liu, L.W., Wang, P.Y., Long, Q.S., Zhao, Y.L., Jin, L.H., Xu, W.M., Chen, Y., Li, Z., Yang, S., 2019. Synthesis and *in vitro* and *in vivo* biological activity evaluation and quantitative proteome profiling of oxadiazoles bearing flexible heterocyclic patterns. J. Agr. Food Chem. 67 (27), 7626–7639. https://doi.org/10.1021/acs.jafc.9b02734.

Tripathi, A., Choubey, P.K., Sharma, P., Seth, A., Tripathi, P.N., Tripathi, M.K., Prajapati, S.K., Krishnamurthy, S., Shrivastava, S. K., 2019. Design and development of molecular hybrids of 2-pyridylpiperazine and 5-phenyl-1,3,4-oxadiazoles as potential multifunctional agents to treat Alzheimer's disease. Eur. J. Med. Chem. 183,. https://doi.org/10.1016/j.ejmech.2019.111707 111707.

Velema, W.A., van der Berg, J.P., Hansen, M.J., Szymanski, W., Driessen, A.J.M., Feringa, B.L., 2013. Optical control of antibacterial activity. Nat. Chem. 5 (11), 924–928. https://doi.org/10.1038/nchem.1750.

Wang, M.W., Zhu, H.H., Wang, P.Y., Zeng, D., Wu, Y.Y., Liu, L.W., Wu, Z.B., Li, Z., Yang, S., 2019. Synthesis of thiazolium-labeled 1,3,4-oxadiazole thioethers as prospective antimicrobials. In Vitro and in vivo bioactivity and mechanism of action. J. Agr. Food Chem. 67 (46), 12696–12708. https://doi.org/10.1021/acs.jafc.9b03952.

Wang, Y.Y., Lu, X.M., Shi, J., Xu, J.H., Wang, F.H., Yang, X., Yu, G., Liu, Z.Q., Li, C.H., Dai, A.L., Zhao, Y.H., Wu, J., 2018. Synthesis andlarvicidal activity of 1,3,4-oxadiazole derivatives containing a 3-chloropyridin-2-yl-1*H*-pyrazole scaffold. Monatsh. Chem. 149 (3), 611–l. https://doi.org/10.1007/s00706-017-2060-3.

Wang, P.Y., Zhou, L., Zhou, J., Wu, Z.B., Yang, S., 2016a. Synthesis and antibacterial activity of pyridinium-tailored 2,5-substituted-1,3,4-oxadiazole thioether/sulfoxide/sulfoxide/sulfone derivatives. Bioorg. Med. Chem. Lett. 26 (4), 1214–1217. https://doi.org/10.1016/j.bmcl.2016.01.029.

Wang, P.Y., Zhou, L., Zhou, J., Wu, Z.B., Xue, W., Song, B.A., Yang, S., 2016b. Synthesis and antibacterial activity of pyridinium-tailored 2,5- substituted-1,3,4- oxadiazole thioether/sulfoxide/sulfone derivatives. Bioorg. Med. Chem. Lett. 26 (4), 1214–1217. https://doi.org/10.1016/j.bmcl.2016.01.029.

Wu, S.K., Shi, J., Chen, J.X., Hu, D.Y., Zang, L.S., Song, B.A., 2021. Synthesis, antibacterial activity, and mechanisms of novel 6-sulfonyl-1,2,4-triazolo[3,4-*b*][1,3,4]thiadiazole derivatives. J. Agr. Food Chem. 69 (16), 4645–4654. https://doi.org/10.1021/acs.jafc.1c01204.

Xiang, J., Liu, D.Y., Chen, J.X., Hu, D.Y., Song, B.A., 2020. Design and synthesis of novel 1,3,4-oxadiazole sulfone compounds containing3,4-dichloroisothiazolylamide moiety and evaluation of rice bacterial activity. Pestic. Biochem. Physiol. 170,. https://doi.org/10.1016/j.pestbp.2020.104695 104695.

Xu, W.M., Yang, S., Bhadury, P., He, J., He, M., Gao, L.L., Hu, D. Y., Song, B.A., 2011. Synthesis and bioactivity of novel sulfone derivatives containing 2,4-dichlorophenyl substituted 1,3,4-oxadiazole/thiadiazole moiety as chitinase inhibitors. Pestic. Biochem. Physiol. 101 (1), 6–15. https://doi.org/10.1016/j.pestbp.2011.05.006.

Yang, L., Ding, W., Xu, Y.Q., Wu, D.S., Li, S.L., Chen, J.N., Guo, B., 2016. New insights into the antibacterial activity of hydroxycoumarins against *Ralstonia solanacearum*. Molecules 21 (4), 468. https://doi.org/10.3390/molecules21040468.

Zeng, D., Wang, M.W., Xiang, M., Liu, L.W., Wang, P.Y., Li, Z., Yang, S., 2020. Design, synthesis, and antimicrobial behavior of novel oxadiazoles containing various *N*-containing heterocyclic pendants. Pest Manag. Sci. 76 (8), 2681–2692. https://doi.org/10.1002/ps.5814.

Zhao, L.J., Duan, F.X., Gong, M., Tian, X., Guo, Y., Jia, L., Deng, S., 2021. (+)-Terpinen-4-ol inhibits *Bacillus cereus* biofilms formation by upregulating the interspecies quorum sensing signals diketopiperazines and diffusing signaling factors. J. Agr. Food Chem. 69 (11), 3496–3510. https://doi.org/10.1021/acs.jafc.0c07826.

Zheng, Y.T., Zhang, T.T., Wang, P.Y., Wu, Z.B., Zhou, L., Ye, Y.Q., Zhou, X., He, M., Yang, S., 2017. Synthesis and bioactivities of novel 2-(thioether/sulfone)-5-pyrazolyl-1,3,4-oxadiazole derivatives. Chin. Chem. Lett. 28 (2), 253–256. https://doi.org/10.1016/j.cclet.2016.06.055.

Zhou, J.W., Ruan, L.Y., Chen, H.J., Luo, H.Z., Jiang, H., Wang, J.S., Jia, A.Q., 2019. Inhibition of quorum sensing and virulence in *Serratia marcescens* by hordenine. J. Agr. Food Chem. 67 (3), 784–795. https://doi.org/10.1021/acs.jafc.8b05922.

Zhou, L., Wang, P.Y., Zhou, J., Shao, W.B., Fang, H.S., Wu, Z.B., Yang, S., 2017. Antimicrobial activities of pyridinium-tailored pyrazoles bearing 1,3,4-oxadiazole scaffolds. J. Saudi Chem. Soc. 21 (7), 852–860. https://doi.org/10.1016/j.jscs.2017.04.005.

Zhu, J.J., Wang, P.Y., Long, Z.Q., Xiang, S.Z., Zhang, J.R., Li, Z.X., Wu, Y.Y., Shao, W.B., Zhou, X., Liu, L.W., Yang, S., 2022. Design, synthesis, and biological profiles of Novel 1,3,4-oxadiazole-2-carbohydrazides with molecular diversity. J. Agr. Food Chem. 70 (9), 2825–2838. https://doi.org/10.1021/acs.jafc.1c07190.

Zhu, H.H., Zeng, D., Wang, M.W., Wang, P.Y., Yang, S., 2019. Integration of naturally bioactive thiazolium and 1,3,4-oxadiazole fragments in a single molecular architecture as prospective antimicrobial surrogates. J. Saudi Chem. Soc. 24 (1), 127–138. https://doi.org/10.1016/j.jscs.2019.10.002.